 CMES, vol.2, no.2, pp.227-236, 2001

An Innovative Open Boundary Treatment for Nonlinear Water Waves in a Numerical Wave Tank

S.-P. Zhu [1]

Abstract: Problems defined on infinite domains must be treated on a finite computational domain. The treatment of the artificially placed boundaries (usually referred to as open boundaries) of such domain truncations can be quite subtle; an over truncation would normally result in large, undesirable reflection of signals back to the computational domain whereas an under truncation would imply an injudicious use of computational resources. In particular, problems occur when strongly nonlinear free surface waves generated in a numerical wave tank are passing through such an open boundary.
In this paper, some recent numerical test results of an innovative treatment of open boundaries are presented. One of popularly adopted techniques of minimizing wave reflections at open boundaries is to use an "absorbing beach", over which wave energy is dissipated. In addition to a kinetic energy based dissipation term traditionally added to the dynamical boundary condition to form an "absorbing beach", a potential energy based term is added, tested and compared with the case of kinetic energy dissipation alone. Our numerical results show that the newly added dissipation mechanism can dissipate energy more effectively over an absorbing beach and consequently result in a much less reflection of wave energy back to the computational domain.

keyword: Open boundary conditions, absorbing beach, nonlinear water waves

1 Introduction

In engineering and applied sciences, there are many problems that are modeled mathematically on an infinite domain as it is simpler sometimes to demand the physical properties to be modeled have certain behaviour at infinity rather than to work out some very specific boundary conditions defined on some given boundaries. However, unless analytical solutions can be worked out for the formed governing differential system, such type of mathematical simplification at the modeling stage may become a burden for a modeler when the formulated problem needs to be solved numerically; the infinite domain must be truncated to a finite computational domain again before a computer can be utilized to solve the problem numerically. Mathematically, this poses a new type of problems: to place an artificial boundary and impose appropriate boundary conditions or some type of treatment immediately behind the open boundary so that the problem can now be computed on a finite domain. The treatment of the artificially placed boundaries (usually referred to as open or fictitious boundaries) of such domain truncations can be quite subtle; an over truncation would normally result in large, undesirable reflection of signals back to the computational domain whereas an under truncation would imply an injudicious use of computational resources. In particular, problems occur when strongly nonlinear free surface waves generated in a numerical wave tank are passing through such an open boundary.

Several different types of treatment have been proposed in the past. In wave diffraction and refraction problems, a commonly adopted technique is to make some further assumption or simplification from the fictitious boundary to the infinity so that eigenfunctions of a linear problem in the outer region can be found and matched with the inner solution on the fictitious boundary [Houston (1981), Tsay and Liu (1983)]. The behaviour of the unknown function at infinity is usually well represented by the eigenfunctions. However, the matching of the inner and outer solution on the fictitious boundary may still create reflections, particularly when the inner solution is highly nonlinear.

A Sommerfeld-type of radiation condition was proposed by Orlanski (1975) for hyperbolic flow problems. Chapman (1985) discussed various forms of the Orlanski conditions; implicit version of the Orlanski conditions seems to perform better, overall, in comparison with its explicit

[1] School of Mathematics and Applied Statistics, The University of Wollongong, Wollongong, NSW 2522, Australia

counterpart. However, the requirement of evaluating the local phase velocity impedes the usage of this type of approaches.

Absorbing beaches (or they are sometimes referred to as "sponges") are another type of techniques used to ensure minimum reflection back to the computational domain once an infinite domain is truncated. Artificial damping (dissipation) is introduced within a finite zone (called an "absorbing beach" or a "sponge") beyond a finite computational domain. The challenge here is to choose a right form of dissipation and beach length to minimize the reflection while maximize the computational efficiency. Betts and Mohamad (1982) added a "damping" term to the free surface dynamic boundary condition while Baker, Merion and Orszag (1981) and Cointe, Geyer, King, Molin and Tramoni (1990) added damping to both dynamic and kinematic boundary conditions. On the other hand, some people even argued [Chapman (1985)] that the combination of a radiation condition and an absorbing beach would have the best damping effect. For example, Ohyama and Nadaoka (1991) and (1994) used friction damping in conjunction with a Sommerfeld-type radiation boundary condition at the lee side of the sponge layer placed at the end of their numerical tank. However, it is not clear that how a radiation condition which is supposed to filter only one frequency can be applied in conjunction with the "absorbing beach" technique, which is capable of damping a wild range of frequencies.

Grilli and Horrillo (1994) proposed that the added surface pressure term along the dissipation beach be proportional to the product of the free-surface normal velocity and the free surface elevation. They calculated the propagation of periodical waves over a numerical tank of constant water depth and also the shoaling of periodic waves over a constant slope and found that the proposed dissipation term works better for short waves than for long waves.

In this paper, we shall concentrate on the "absorbing beach" technique and present some recent numerical test results of an innovative damping term added to the dynamic boundary condition. The work is primarily based on Cao, Beck and William (1993). However, instead of having a term dissipating kinetic energy, we found that adding a term that is of the form of potential energy made a significant difference in terms of reflection. Our numerical results show that the newly added dissipation mechanism can dissipate energy more effectively over an absorbing beach and consequently result in a much less reflection of wave energy back to the computational domain.

This paper is subdivided into 5 sections. In Section 2, we shall outline the numerical approaches for simulating the nonlinear waves. In Section 3, we shall present our absorbing beach with a new dissipation term added. In Section 4, a test problem based on a benchmark test at ISOPE98 Montréal Conference and some preliminary numerical results are presented and discussed. Our concluding remarks are given in Section 5.

2 The Desingularized Boundary Integral Method

For water wave problems, we solve, at each time step, a mixed boundary value problem of

$$\begin{cases} \triangle\phi = 0 & (\text{in } \Omega) \\ \phi(\xi,\mathbf{x}) = \phi_0 & (\text{in } \Gamma_f) \\ \frac{\partial\phi}{\partial n} = q_0 & (\text{in } \Gamma_s) \end{cases} \tag{1}$$

where ϕ is the wave potential, $\triangle$ is the Laplacian operator, Ω is the domain occupied by water, Γ_f is the free surface and ϕ_0 is a known function resulting from the updating of potential function values on the free surface at each time step; q_0 is the prescribed normal derivative on a solid boundary Γ_s (usually it is the normal velocity of the solid boundary). Although the governing equation is linear and time independent, the problem is highly nonlinear and time dependent as the position of the free surface, which advances with time, is part of the solution and the dynamic boundary condition imposed on the free surface is usually nonlinear. The kinematic boundary condition, which is used to advance the position of the free surface and the dynamic boundary conditions will be discussed in the next section.

With the well known free-space fundamental solution of the Laplace operator

$$\phi^* = \frac{1}{2\pi}\ln\frac{1}{|\mathbf{x}-\xi|},$$

an integral equation

$$\begin{aligned} c(\xi)\phi(\xi) + \int_{\Gamma_s}\phi(\mathbf{x})q^*(\xi,\mathbf{x})d\Gamma(\mathbf{x}) - \int_{\Gamma_f}q(\mathbf{x})\phi^*(\xi,\mathbf{x})d\Gamma(\mathbf{x}) \\ = \int_{\Gamma_s}q_0(\mathbf{x})\phi^*(\xi,\mathbf{x})d\Gamma(\mathbf{x}) - \int_{\Gamma_f}\phi_0(\mathbf{x})q^*(\xi,\mathbf{x})d\Gamma(\mathbf{x}) \end{aligned} \tag{2}$$

can be easily derived for any source point ξ, using either Green's second identity or integration by parts twice. In Eq. (2), $\mathbf{x}$ is a so-called field point, with respect to which the surface integral is carried out, and $c(\xi)$ is geometric parameter depending of the location of ξ (for 2D problems):

$$c(\xi) = \begin{cases} 1 & \text{if } \xi \in \Omega \\ \frac{1}{2} & \text{if } \xi \in \Gamma_f \cup \Gamma_s \\ 0 & \text{if } \xi \notin \Omega \cup \Gamma_f \cup \Gamma_s. \end{cases}$$

If the source points are chosen to be on the boundary $\Gamma_f \bigcup \Gamma_s$, this results in a traditional boundary integral equation, the solution of which requires the treatment of the singularity when the field point $\mathbf{x}$ coincides with the source point ξ. As pointed out by Cao, Beck and William (1991), the numerical calculations can be quite costly for the evaluation of a singular integrand, especially for time-dependent non-linear free surface problems.

One way of avoiding the evaluation of singular integrand is to let the source point ξ be located outside of the boundary $\Gamma_f \bigcup \Gamma_s$. Then, Eq. (2) becomes

$$\begin{aligned} &\int_{\Gamma_s} \phi(\mathbf{x}) q^*(\xi,\mathbf{x}) d\Gamma(\mathbf{x}) - \int_{\Gamma_f} q(\mathbf{x}) \phi^*(\xi,\mathbf{x}) d\Gamma(\mathbf{x}) \\ &\quad = \int_{\Gamma_s} q_0(\mathbf{x}) \phi^*(\xi,\mathbf{x}) d\Gamma(\mathbf{x}) - \int_{\Gamma_f} \phi_0(\mathbf{x}) q^*(\xi,\mathbf{x}) d\Gamma(\mathbf{x}) \end{aligned} \tag{3}$$

which is no longer singular and is a Fredholm integral equation of the first kind.

It is usually more difficult to solve a Fredholm equation of the first kind than that of the second kind, mainly because the ill-posed nature of this type of integral equations as pointed out by de Hoog (1980) and many others. Such an ill-posed nature is somehow reflected by the unstable numerical solutions as experienced by many researchers. However, for first-kind equations, if a proper functional space to which the solution belongs to is adopted, the equation system will become properly-posed as pointed out by Baker (1977) and many others. Cao, Beck and William (1991) showed that by properly choosing the characteristic distance by which the source points are placed outside the computational domain, stable and accurate numerical results can be obtained. According to Cao, Beck and William (1991), if these source points are placed too far away from the boundary, the resulting linear algebraic system is poorly conditioned, resulting in large numerical errors. On the other hand, if they are placed too close to the boundary, the integrand is "almost" singular and numerical accuracy is poor too. Cao, Beck and William (1991) proposed a formula for such a distance:

$$L_d = \ell_d (D_m)^{\alpha},$$

where L_d is the smallest distance between a source point and a field point, l_d is a parameter that reflects how far the integral equation is desingularized, D_m is the local mesh size and α is a parameter to be determined by numerical experiments. As recommended by Cao, Beck and William (1991), we chose $l_d = 1$ and $\alpha = 0.5$ in all of our calculations for the results presented in Section 4.

3 New Absorbing Beach

On the free surface, the kinematic boundary condition

$$\frac{D\mathbf{x}}{Dt} = \nabla\phi \tag{4}$$

and dynamic boundary condition

$$\frac{D\phi}{Dt} = -g\eta - \frac{1}{2}\nabla\phi \cdot \nabla\phi \tag{5}$$

are used to advance our calculation at each time step. In Eq. (5), g is the gravitational acceleration and η is the free surface elevation. Eq. (4) is used to advance the free surface to its new position and Eq. (5) is used to advance the velocity potential on the new location of the free surface.

In the zone where artificial damping is switched on (i.e., on the absorbing beach where energy is expected to be "absorbed"), one can add an additional term, P_{damp}, in the dynamic boundary condition:

$$\frac{D\phi}{Dt} = -g\eta - \frac{1}{2}\nabla\phi \cdot \nabla\phi - \frac{P_{damp}}{\rho}, \tag{6}$$

where P_{damp} is some kind of artificial pressure applied on the free surface and ρ is the water density. As pointed out by Cao, Beck and William (1993), the energy absorption rate associated with the damping term is

$$\frac{dE_f}{dt} = \int_{\Gamma_{fb}} P_{damp} \phi_n d\Gamma \tag{7}$$

where ϕ_n denotes the normal derivative of the potential ϕ on Γ_{fb}, which denotes the free surface above the absorbing beach.

There have been various forms of P_{damp} proposed in the literature. $P_{damp} = \nu\phi$ is used in Betts and Mohamad (1982), Baker, Merion and Orszag (1981) and Cointe, Geyer, King, Molin and Tramoni (1990). Such a choice does not guarantee a positive definite kernel in Eq. (7) and consequently the energy may even be "pumped" into the fluid. Cao, Beck and William (1993) suggested that P_{damp} take the form

$$P_{damp} = \nu(x)\text{sign}(\phi_n) \mid Q \mid, \tag{8}$$

where Q can be any function including nonlinear functions of ϕ and/or ϕ_n and $\nu(x)$ is a positive function that allocates different amount of dissipation at each point along the beach. In their numerical tests, they tested two functions with $Q = \phi$ and $Q = \phi_n$ and found that the total energy decay for the case of $Q = \phi_n$ is always monotonic, which indicates that the beach always absorbs energy. On the other hand, For the case of $Q = \phi$, the total energy decay is not alway monotonic. They appeared to favor the former choice more. Subramani, Beck and William (1998) used $Q = \bigtriangledown\phi \cdot \bigtriangledown\phi$ and suggested that their form of energy dissipation works better when waves break. However, they did not directly compare their results with those of Cao, Beck and William (1993).

The current research was motivated by the fact that most of the researchers linked P_{damp} with quantities that are directly associated with the kinetic energy (e.g., velocity potential, normal velocity or even the square of the magnitude of the total velocity on the free surface), no one seems to have linked the P_{damp} with the counterparts of the kinetic energy in this problem, the potential energy. A combination of these two effects being included in the P_{damp} term seems to be so natural as these two forms of energy both appear in the original dynamic boundary condition (5) already. Therefore, we propose that P_{damp} take a more general form

$$\frac{P_{damp}}{\rho} = \nu(x)\text{sign}(\phi_n)[r|\nabla\phi|^2 + (1-r)g|\eta|] \tag{9}$$

where r is the percentage of the contribution of each term and $\nu(x)$ is a function that distributes the dissipation along the beach. When r is equal to 1, the dissipation is purely kinetic energy based as the cases studied before. On the other hand, if r is set to zero, the dissipation becomes purely potential energy based. The objective of this project is to find what is the best combination of these two forms of dissipation in order to render minimum reflection. Test results of a benchmark case is presented in the next section to illustrate the best r values in terms of numerical dissipation on the absorbing beach.

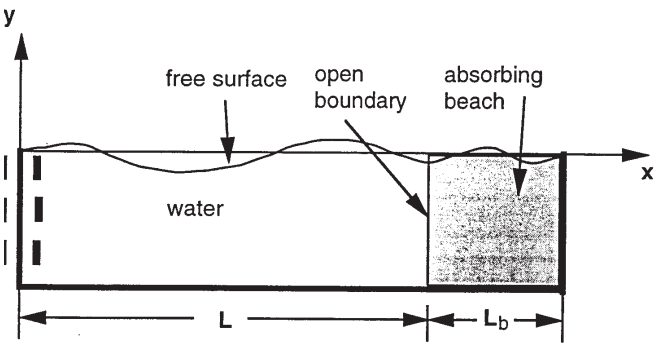

Figure 1 : A sketch of the computational domain and the "absorbing beach".

It should be noted that the proposed P_{damp} is different from that used by Grilli and Horrillo (1994); the one proposed in this paper is clearly based on an energy consideration whereas it is not clear what physically the product of $\frac{\partial\phi}{\partial n}$ and η in Grilli and Horrillo (1994) represents. In addition, it is not guaranteed that the energy is always dissipated along the beach if the form of P_{damp} proposed by Grilli and Horrillo (1994) is taken, since η itself can be positive or negative.

There are several forms of distribution functions (e.g., Cao, Beck and William (1993) and Subramani, Beck and William (1998)). But, all these distribution functions have a common feature; it is equal to zero at the beginning of the beach and monotonically increase along the beach. In order to focus on the dissipation mechanism rather than the optimal distribution of dissipation, we adopted the distribution function used in Cao, Beck and William (1993), i.e.,

$$\nu(x) = \nu_0(\frac{x-L}{L_b})^2, \tag{10}$$

for all the results presented in the next section. In Eq. (10), ν_0 gives the strength of the overall dissipation and will be referred to as the beach strength from now on.

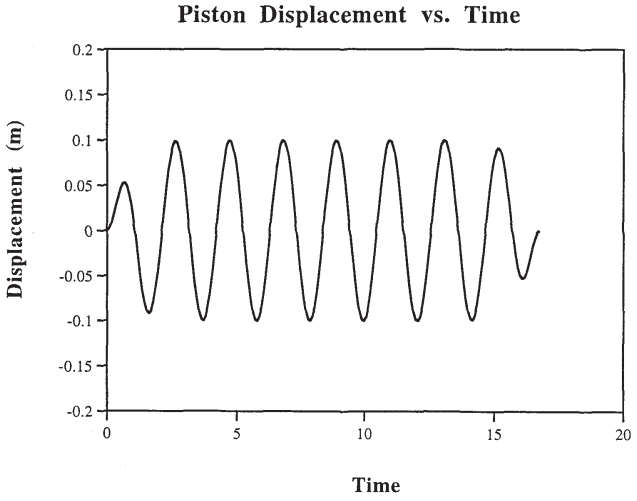

Figure 2 : Displacement of the wavemaker.

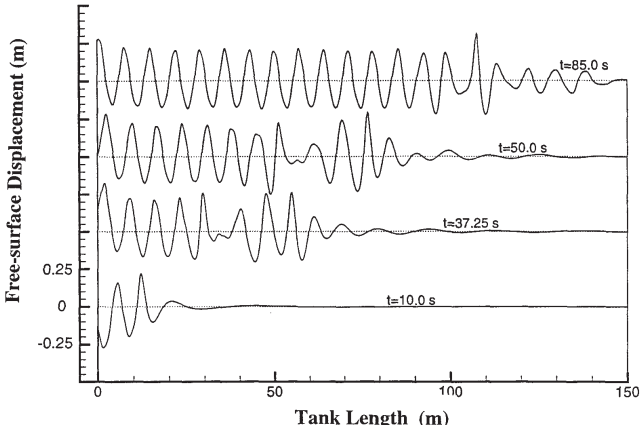

Figure 3 : Free surface elevations at different time steps: (a) at $t = 10$ s; (b) at $t = 37.25$ s; (c) at $t = 50$ s; (d) at $t = 85$ s.

4 Numerical Test Results and Discussions

At its ISOPE98 Montréal conference, the International Society for Offshore and Polar Engineering set up a series of benchmark problems to test the numerical absorption of outgoing waves in numerical tanks. The purpose of these benchmark tests seems to match our objective quite well, i.e., to avoid wave reflection and make the open boundary of a numerical wave tank as transparent to the incoming waves as possible.

We adopted one of these benchmark problems in a numerical wave tank to test our new dissipation terms. As illustrated in Fig. 1, the tank is 9.81 m high and 58.86 m long. Although the physical dimension of the tank can be given other values so long as the ratio of these two is equal to 6 as required in the benchmark problem, we chose these two numbers so that the ratio of $\frac{g}{h} = 1s^{-2}$. On the right hand side of the tank, an absorbing beach of various beach length is placed at the exit of the numerical tank. On the left hand side of the tank, a piston wavemaker, the position of which is prescribed by

$$x = A\tanh(t)\sin(\omega t)\tanh(n\frac{2\pi}{\omega} - t), \tag{11}$$

is located at the left end of the tank. In Eq. (11), A is the amplitude, ω is the angular frequency, t is time and n is the number of periods in the wave packet. The motion of the piston within a typical packet is depicted in Fig. 2.

It was recommended that the dimensionless wave amplitude be taken as 0.012 (non-dimensionalized by the mean water depth). For the wave tank we took, this is equivalent to 0.11772 m. However, when we tried to establish a solution with a sufficiently long tank (such a solution is needed in order to check the amount of reflection of each beach under test), we found that with this amplitude, nonlinear waves always break before the recommended simulation time of 85 s is reached no matter how long the tank is. Therefore, we had a choice of either taking a short simulation time or a sightly smaller amplitude. We chose the latter as we felt that so long as the amplitude of the piston is large enough to generate highly nonlinear waves, it would serve the objective of this study. On the other hand, if we had shorten the simulation time, the dissipation effect of a beach might not have been fully explored before the simulation is over.

Four free surface positions corresponding to $t = 10$, $t = 37.25$, $t = 50$ and $t = 85$ s are respectively shown in Fig. 3, with a beach length of 91.14 m (a total length of 150 m), which is more than one and half times of the tank length. Here, ω was chosen to be 8 s^{-1} and $n = 8$ as suggested in the benchmark test guideline. As one can see, waves in the test section are indeed highly nonlinear as they evolve with the time. This is the solution that we are going to regard as the "true" solution so that all the other solutions with various beach lengths and dissipation mechanisms can be tested against. The reason we chose the solution corresponding to a total length of 150 m was because there was very little change in the test section once the total length passes beyond 120 m. We also varied the dissipation strengths to make sure that less than 0.5% of changes in the test section were found.

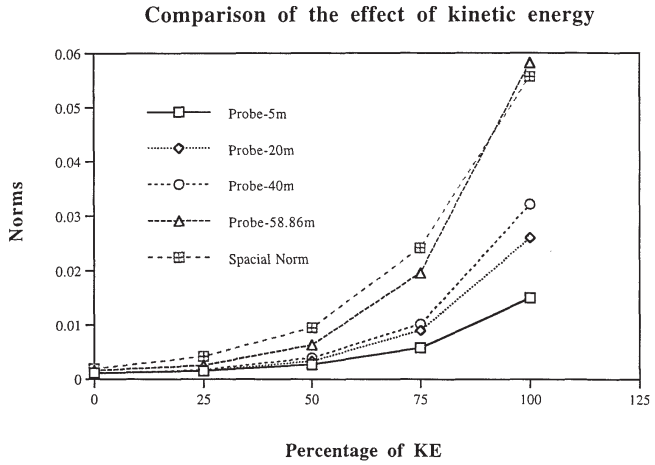

Figure 4 : Variation of norms vs. KE/PE ratio.

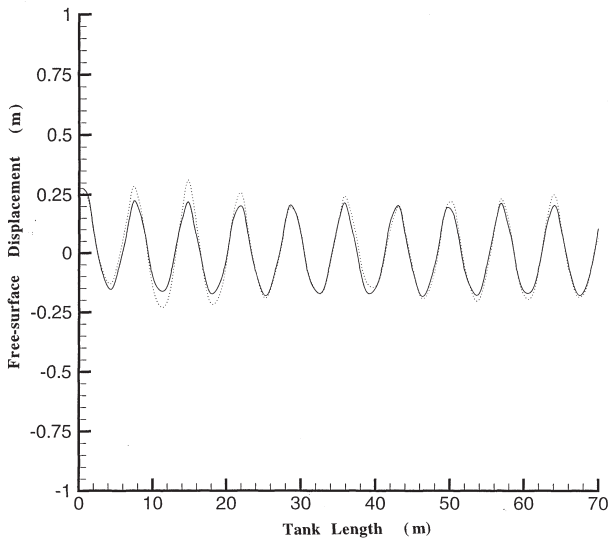

Figure 5 : Comparison of free surface elevations when KE/PE ratio is 100%.

Using this "true" solution, we can now define some L_2 norms to measure the transparency of the open boundary. To measure the temporal difference of the free-surface elevation at a specific location i, we let

$$N_i = \frac{\sum_{m=1}^{M} (\eta_m^{(i)} - \eta_m^{(ir)})^2}{\sum_{m=1}^{M} \eta_m^{(ir)2}}, \tag{12}$$

where M is the total number of time steps included in the norm, $\eta_m^{(i)}$ is the free-surface elevation of a test at the time step m and at the probe location i and $\eta_m^{(ir)}$ is the corresponding free-surface elevation of the "true" solution at same time and location. To measure the spatial differences of a test case with that of the "true" solution, we let

$$N_s = \frac{\sum_{m=1}^{M}\sum_{n=1}^{N} (\eta_{mn}^{(i)} - \eta_{mn}^{(ir)})^2}{\sum_{m=1}^{M}\sum_{n=1}^{N} \eta_{mn}^{(ir)2}}, \tag{13}$$

where the subscripts mn denote the corresponding quantity being measured at mth time step and at the nth nodal point.

Five probes were placed in the wave tank to record the time series of the free surface elevation. Four of these were placed at 5, 20, 40 and 58.86 m locations and one was at the end of the "absorbing beach". It is expected that in general the reflection of waves should increase if one moves towards the open boundary placed at 58.86 m. For a given dissipation distribution function, there are three variables we can test, the percentage of the kinetic energy term vs. the potential energy term, the beach length and the beach strength.

Fig. 4 shows the variations of N_i norms ($i = 1,2,3,4$) and N_s norm in terms of different proportion of kinetic and potential energies when the beach strength and the beach length are fixed at $\nu_0 = 1.0$ and $L_b = 12$ m, respectively. Clearly shown is the small difference between the solution with 12 m beach and that of the "true" solution at location closer to the wavemaker (e.g., at the 5 m probe) for a given KE/PE (kinetic energy/potential energy) ratio. Such difference increases as the probe location gets closer to the open boundary. In other words, reflections from the open boundary decays as one moves away from it, which is as expected. The most interesting is that all the norms monotonically decrease when the component of potential energy dissipation becomes larger. For 100% potential energy, the N_s norm reaches about 0.0019, which is more than 30 times less than that of 100% kinetic energy. This is a significant improvement!

The N_s for the case of 100% kinetic energy is equal to 0.057. To have a feeling of what the difference of the free surface elevations this amount of norm is equivalent to, we ploted out the comparison of the free surface elevation at the last moment of our simulation, i.e., $t = 85$

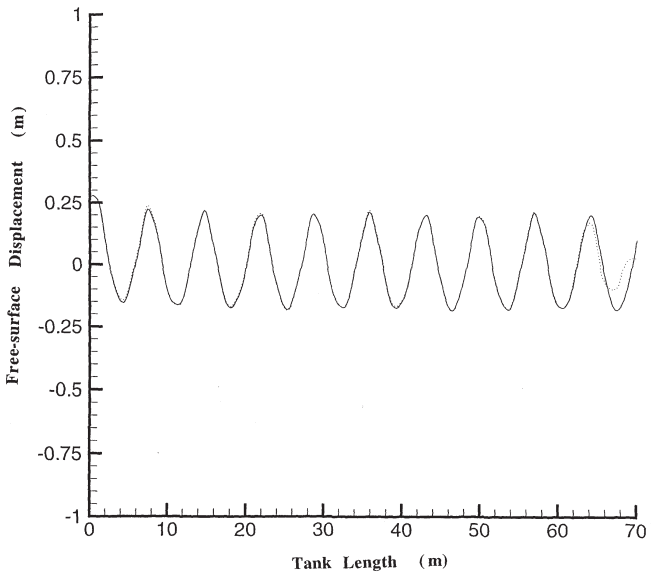

Figure 6 : Comparison of free surface elevations when KE/PE ratio is 0%.

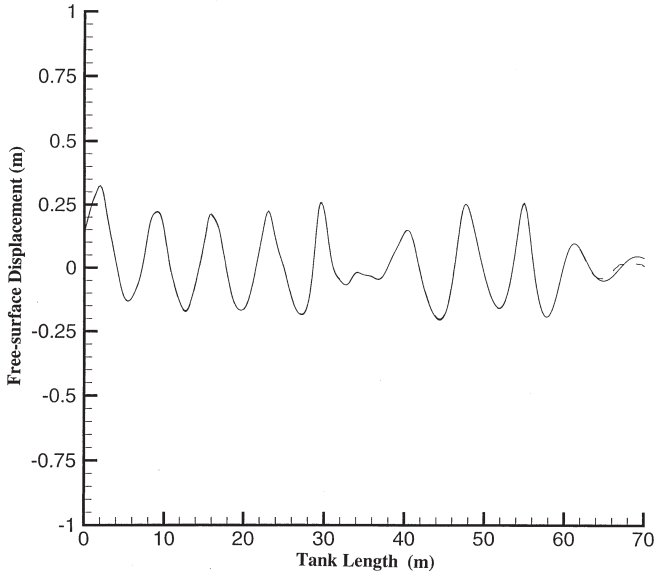

Figure 7 : Comparison of free surface elevations when KE/PE ratio is 0%.

s, in Fig. 5. As one can see, the difference between the solution of a 12 m beach and that of the "true" solution is quite large. On the other hand, for the case of 100% potential energy, such a difference is considerably small as shown in Fig. 6. For any time before the end of simulation, the difference is even smaller. Fig. 7 shows the difference between the solution of a 12 m beach and that of the "true" solution at $t = 37.25$ s. Clearly, one can hardly tell any difference between the two curves, except in the beach zone.

One must have also observed that the difference becomes large in Figs. 5-7 on the beach between $x = 58.86$ and $x = 70.86$. This clearly shows that the effect of the dissipation on the beach. As the strength of the dissipation increases towards the end of the beach, so did the differences between the free surfaces there. Once again, this is what we expected. What we didn't expect was that for the quadratic distribution function, the potential energy term appears to work best alone, in terms of minimum reflection or the transparency of the open boundary.

For beach strength ν_0, what we like is a reasonably large range of ν_0, within which the norms don't change too much. In other words, we would like to identify a range of ν_0, within which the results are insensitive to the selection of ν_0. This is because once we have found an optimal beach profile in terms of its dissipation strength, beach length, the ratio of potential energy vs. kinetic energy, and strength distribution, we would not like them to be problem dependent.

Figs. 8, 9 and 10 show the variations of 5 norms vs. the beach strength ν_0 when the beach length is fixed at 12 m and the percentage of the kinetic energy is fixed at 0, 50 and 100, respectively. For the case that the percentage of the kinetic energy dissipation is 50 and 100, around $\nu_0 = 2$ clearly appears to be the optimal value. However, for the case that the percentage of the kinetic energy dissipation is 0, the spatial norm corresponding to $\nu_0 = 2$ is actually slightly larger than those when $\nu_0 = 1$ and $\nu_0 = 3$ while the other four temporal norms are still the lowest at $\nu_0 = 2$. Therefore, we can safely recommend $\nu_0 = 2$. More importantly, one should notice that there is indeed a reasonably wide range of ν_0 such that these norms remain low. Such a range shifts a little bit from $1 < \nu_0 < 3$ for KE/PE ratio being 100 and 50 to $2 < \nu_0 < 4$ for KE/PE ratio being 0. Therefore, it is believed that choosing ν_0 around 2 would yield the minimum reflection.

Another aspect is of course the influence of the beach length. Naturally, we expect that the longer the beach length is, the more energy will be absorbed and consequently resulting in less reflection. On the other hand, longer beach of course increase the computational expenses in terms of both data storage and CPU time. It is certainly a great advantage if we can find a guideline for the ratio of the beach length to that of the wave tank.

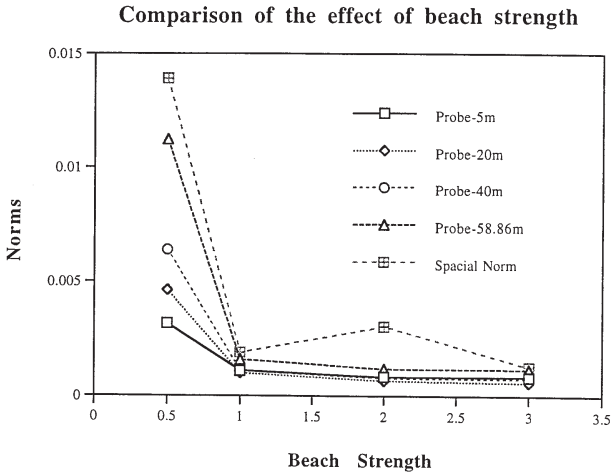

Figure 8 : Variation of norms vs. beach strength ν_0 when KE/PE ratio is 0%.

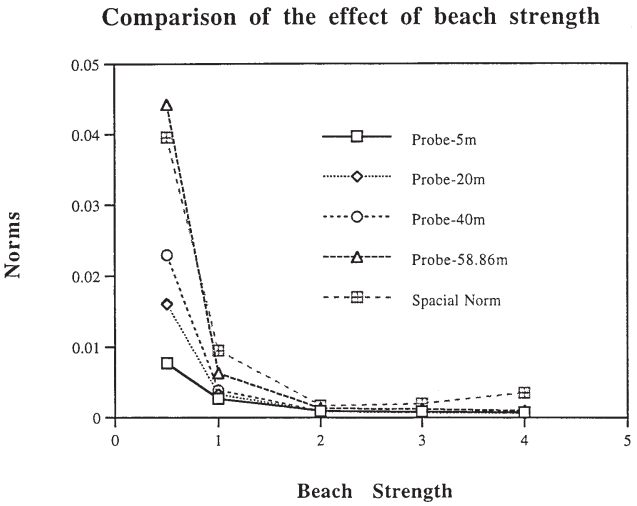

Figure 9 : Variation of norms vs. beach strength ν_0 when KE/PE ratio is 50%.

Figs. 11, 12 and 13 show the variations of 5 norms vs. the beach length when the beach strength $\nu_0 = 1$ and the percentage of the kinetic energy is fixed at 0, 50 and 100, respectively. Clearly, a 3 m beach would be too short for all cases (for KE/PE ratio being 0, the errors were so big that we could not even plot it out). Beach length of 6 m still renders reasonably good results as shown in Fig. 14, in which the comparison of free surface elevation from $L_b = 6$ to that of the "true" solution is plotted. Our other sets of data display some similar behaviour. Therefore, a 10 to 20% beach length to that of the tank length is recommended.

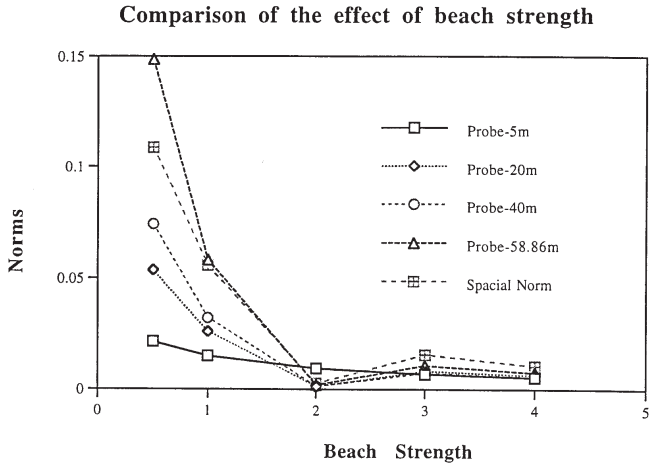

Figure 10 : Variation of norms vs. beach strength ν_0 when KE/PE ratio is 100%.

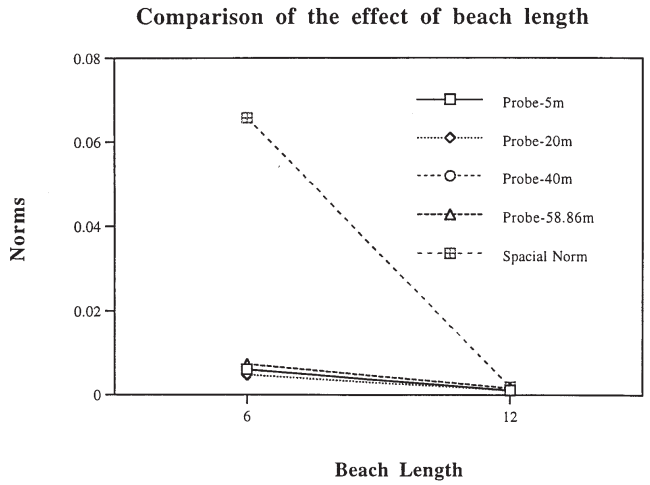

Figure 11 : Variation of norms vs. beach length L_b when KE/PE ratio is 0%.

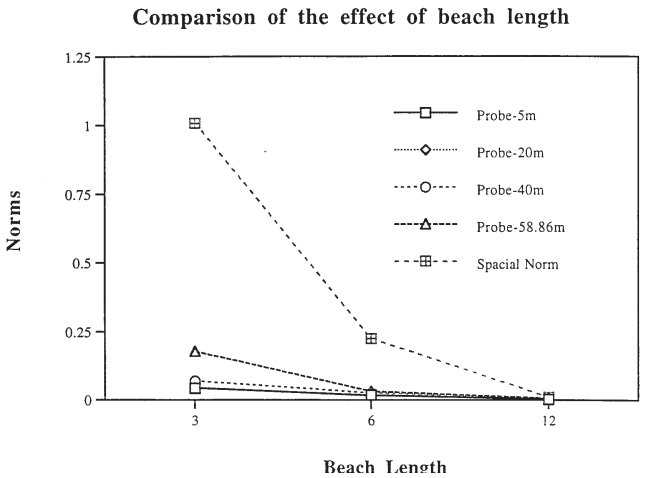

Figure 12 : Variation of norms vs. beach length L_b when KE/PE ratio is 50%.

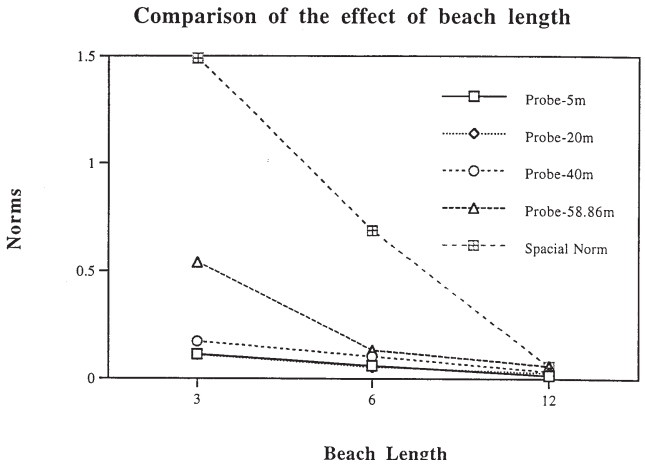

Figure 13 : Variation of norms vs. beach length L_b when KE/PE ratio is 100%.

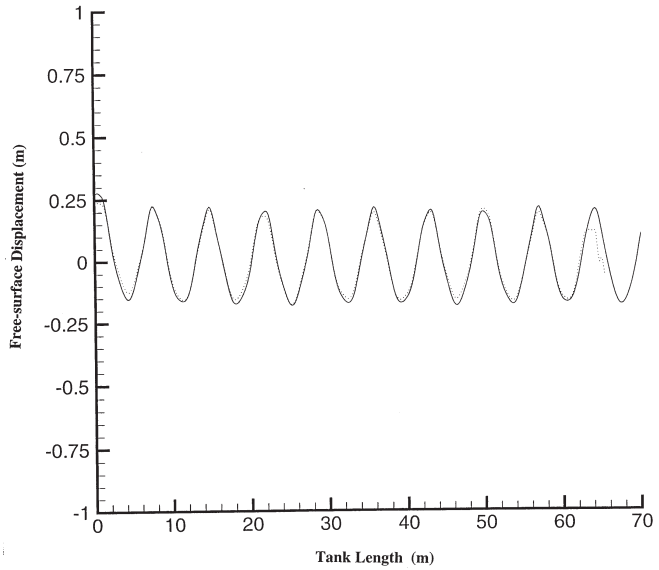

Figure 14 : Comparison of free surface elevations when KE/PE ratio is 0%.

5 Conclusions

In this paper, a new dissipation term is proposed to be added to the dynamic boundary condition on an "absorbing beach" in order to minimize the wave reflection due to the truncation of an infinite domain to a finite one. Our numerical test results show that the newly proposed potential energy based dissipation term indeed works better in comparison with the previously adopted kinetic energy based dissipation term. It is recommended that the beach strength take a value of $\nu_0 = 2$ and beach length take about 10 to 20% of the numerical tank length under study.

Acknowledgement: The author would like to thank Prof. W. W. Schultz of the Department of Mechanical Engineering and Applied Mechanics, The University of Michigan for many inspiring discussions while he spent his sabbatical leave at the University of Michigan and Mr. A. K. Subramani of the Department of Naval Architecture and Marine Engineering, The University of Michigan for his generous and patient help to familiarize the author with the local computer system and many useful suggestions on the manuscript. Ms. C. Silveri's help in typesetting the final version of this paper is also gratefully acknowledged.

Reference

Baker, C. T. H. (1977): *The numerical treatment of integral equations*, Claredon Press 635-645.

Baker, G. R.; Merion, D. I.; Orszag, S. A. (1981): Applications of a Generalized Vortex Method to Nonlinear Free Surface Flows, *Proceedings of 3rd International Conference on Numerical Ship Hydrodynamics*, 179-191.

Betts, P. L.; Mohamad, T. T. (1982): Water Waves: A Time-Varying Unlinearized Boundary Element Approach, *Proc. 4th Int. Symp. on Finite Element Methods in Flow Problems*, 923-929.

Cao, Y.; Beck, R. F.; William, W.W. (1991): Three-dimensional desingularized boundary integral methods for potential problems, *Int. J. For Num. Methods in Fluids*, 785-803.

Cao, Y.; Beck, R. F.; William, W.W. (1993): Absorbing beach for numerical simulation of nonlinear waves in a wave tank, *8th Int. WWWFB*, 16-19.

Chapman, D. C. (1985): Numerical Treatment of Cross-Shelf Open Boundaries in a Barotropic Coastal Ocean Model, *J. Phys. Oceanography*, **15** 1060-1075.

Cointe, R.; Geyer, P.;King, B.; Molin, B.; Tramoni, M.-P. (1990): Nonlinear and Linear Motions of a Rectangular Barge in a Perfect Fluid, *Proceedings of 18th Symposium on Naval Hydrodynamics*, 85-99.

de Hoog, F. (1980): Review of Fredholm Equations of the first kind, *The application and numerical solution of integral equations*, edited by R. S. Anderssen, F. R. de

Hoog and M. A. Lukas, 119-134.

Grilli, S.; Horrillo, J. (1994) Numerical Generation and Absorption of Fully Nonlinear Periodical Waves, *J. of Eng. Mech.-ASCE*, **123(10)** 1060-1069.

Houston, J.R. (1981): Combined refraction and diffraction of short waves using the finite element method, *Applied Ocean Research*, **3**, 163.

Ohyama, T.; Nadaoka, K. (1991): Development of a nonlinear wave tank for analysis of nonlinear and irregular wave field, *Fluid Dyn. Res*, **8**, 231-251.

Ohyama, T.; Nadaoka, K. (1994): Transformation of a nonlinear wave train passing over a submerged shelf without breaking, *Coastal Engineering*, **24**, 1-22.

Orlanski, I. (1975): A simple boundary condition for unbounded hyperbolic flow, *J. Comput. Phys.*, **21**, 251-269.

Subramani, A.; Beck, R. F.; William, W.W. (1998): Suppression of wave-breaking in nonlinear water wave computations, *Proceedings of 13th International Workshop on Water Waves and Floating Bodies*, 135-139.

Tsay, T.-K.; Liu, P. L.-F. (1983): A finite element model for wave refraction and diffraction, *Applied Ocean Research*, **5**, 30-37.